In Pursuit of New Real-Time Ancillary Services Providers: Hidden Opportunities in Low Voltage Networks and Sustainable Buildings

Iason-Iraklis Avramidis, *Student Member, IEEE*, Florin Capitanescu, *Member, IEEE*, Vasileios A. Evangelopoulos, Pavlos S. Georgilakis, *Senior Member, IEEE*, and Geert Deconinck, *Senior Member, IEEE*

***Abstract*—Following recent EU directives, the penetration of smart sustainable buildings (SSBs) in low voltage (LV) networks is expected to drastically increase. This open ups opportunities for developing novel frameworks to coordinate the provision of ancillary services (AS) stemming from SSBs. In pursuit of investigating the extent of the previously untapped potential of LV networks, this work proposes, for the first time, the development of an SSB-driven MV-LV coordination framework for the provision of AS, inspired by industrial HV-MV AS schemes from the European landscape. Analytical formulations of passive and active ancillary schemes are first presented, in the form of mixed-integer nonlinear programming problems. Analytical reformulations and approximations are then proposed, to derive computationally lighter mixed-integer linear programming models. The real-time management of AS provision is based on a novel 3-stage, model predictive control approach, driven by the collaboration between distribution system operator and SSBs, the latter considering environmental and phase balancing aspects in their optimizations. Emergency situations with network violations are also considered. The approach is validated, tested, and compared to its predecessor, i.e., its past, cruder version, on a multi-feeder LV network containing different types of SSBs.**

***Index Terms*—Ancillary services, low voltage networks, model predictive control, smart sustainable buildings.**

NOMENCLATURE

Sets

$\mathcal{B}$	Set of smart sustainable buildings (SSB, index b)
$\mathcal{E}$	Set of electric vehicles (EV, index e)
$\mathcal{F}$	Set of flexible loads (FL, index f)
$\mathcal{I}$	Set of nodes (indices i, j)
$\mathcal{P}$	Set of photovoltaics (PV, index p)
$\mathcal{T}$	Set of time periods (index t)
$\mathcal{Z}$	Set of phases (index z).

Parameters (Network/DSO & Buildings)

a, b, c	Linear factors for piecewise flow limit approximation
$C^{\checkmark}$	Compliance reward, active scheme (€/kVar)
C^{x}	Non-compliance penalty, active scheme (€/kVar)
C^{P}	Zones 2 and 3 penalty, passive scheme (€/kVar)
g, b	Line susceptance/conductance (p.u.)
M	Big-M parameters for ancillary services schemes
P^{actual}	Actual active power of building (kW)
P^{fixed}	Fixed active power of non-smart buildings (kW)
P^{min}	Active power MV-LV exchange limit, passive scheme, when adaptive reactive limit "kicks-in" (kW)
P^{rate}	Rated power for PV or EV (kW)
Q^{actual}	Actual reactive power of building (kVar)
Q^{fixed}	Fixed reactive power of non-smart buildings (kVar)
Q^{min}	Minimum reactive power MV-LV exchange limit, passive scheme (kVar)
$R^{\mathrm{P,max}}$	Active power request ramp limit (kW/period)
$R^{\mathrm{Q,max}}$	Reactive power request ramp limit (kVar/period)
S^{gen}	PV generated apparent power (kVA)
V^{set}	Desired substation voltage (p.u.)
ϵ	Voltage deviation tolerance for active scheme (%)
ι	Vector of approximated voltage magnitudes and angles for the piecewise power flow linearization.

Variables (Network/DSO & Buildings)

P^{ex}	MV-LV exchanged active power (kW)
P^{inj}	PV injected active power (kW)
P^{R}	DSO-requested active power (kW)
Q^{ex}	MV-LV exchanged reactive power (kVar)
Q^{inj}	PV injected reactive power (kVar)
Q^{lim}	Exchange limit of reactive power at MV-LV (kVar)
Q^{R}	DSO-requested reactive power (kVar)
V^{m}	Measured voltage at substation secondary side (p.u.)
ΔP^{+}	DSO request for active power increase (kW)

Manuscript received April 21, 2021; revised July 4, 2021; accepted September 13, 2021. Date of publication September 15, 2021; date of current version December 23, 2021. This work was supported by the Luxembourg National Research Fund (FNR) in the framework of gENESiS Project under Grant C18/SR/12676686. Paper no. TSG-00632-2021. *(Corresponding author: Iason-Iraklis Avramidis.)*

Iason-Iraklis Avramidis and Florin Capitanescu are with the Environmental Research and Innovation, Luxembourg Institute of Science and Technology, 4362 Esch-sur-Alzette, Luxembourg (e-mail: jasonavra@yahoo.com).

Vasileios A. Evangelopoulos and Pavlos S. Georgilakis are with the School of Electrical and Computer Engineering, National Technical University of Athens, 15780 Athens, Greece.

Geert Deconinck is with ESAT-ELECTA, Katholieke Universiteit Leuven, 3001 Leuven, Belgium.

Color versions of one or more figures in this article are available at https://doi.org/10.1109/TSG.2021.3112925.

Digital Object Identifier 10.1109/TSG.2021.3112925

ΔP^{-}	DSO request for active power decrease (kW)
ΔQ^{+}	DSO request for reactive power increase (kVar)
ΔQ^{-}	DSO request for reactive power decrease (kVar)
$\sigma^{\text{ov,uv}}$	Violation of upper/lower voltage limit (p.u.)
σ^{cg}	Violation of line thermal limit (p.u.)
Ψ	Binary variables for ancillary services schemes.

I. Introduction

THE EU has taken an active role in influencing the power grid's transition to an active and sustainable entity. A major pillar of innovation is the promotion of smart sustainable buildings (SSBs) and of their large-scale integration [1]. Besides comprising a variety of smart distributed energy resources (DERs), SSBs balance out their yearly consumption and on-site renewable production, constituting nearly zero energy (nZE) entities. Aside from the undeniable environmental and customer benefits, SSBs can also drastically increase the available flexibility in distribution systems (DS), to combat congestions and voltage issues [2], [3]. However, as that flexibility grows, DS can at times end up with significant amounts of "inert" flexibility. This phenomenon naturally spawned a new, highly relevant research line in power systems: the provision of ancillary services (AS) by active DS [4], [5].

The concept of DS providing flexibility support to higher voltage levels has attracted significant interest, with large-scale, proof-of-concept projects having produced promising results [6]. Currently, research efforts are almost exclusively focused on the interactions between transmission and distribution system operators (TSO-DSO), and how the latter can support the former during planning and operation. Academia seems to have reached some consensus on the best way to implement this cooperation: the derivation and "marketization" of flexibility envelopes, commonly referred to as P-Q charts [7]. While the concept finds application in other areas as well, e.g., virtual power plants [8] and DER [9], its application in flexibility aggregation is the one most commonly encountered.

Despite P-Q charts being a favoured approach for defining a distribution network's flexibility region, computing them in practice is challenging and usually done through approximations, due to the sheer amount of technical considerations that must be taken into account. Challenges include aggregating assets of different variability and temporal characteristics [10], dealing with the impact of strategic decisions from market players, whose interests may negatively affect the DSO [11], dealing with high levels of uncertainty [12], or exploring how local (pre-set) controls, advanced communication infrastructure and DER aggregation can affect or replace such an approach [13]. Furthermore, there is no clear consensus on the appropriate type of control (centralized vs decentralized), the best management approach (rights and obligation of involved parties), or on how to associate each point within the chart with a distinct cost/bid for the aggregated flexibility [14].

Providing ancillary support presupposes that one's own system is free of internal issues. Ancillary support should not be forced, nor should it undermine the DSO's efforts to optimally manage its own system. Some researchers are of the opinion that flexibility "harvesting" should be performed in a bottom-up manner, and that LV networks should individually support the MV grid, so that it may subsequently interact with the TSO reliably, see [15], [16]. Despite the strides that have been made, this area also has obstacles to overcome. Most works on LV network flexibility tend to aggregate resources with disregard of network constraints [17], oversize energy devices [18], employ sensitive data-driven approaches [19], or assume complete controllability of the network [20]. Active aggregators managing LV networks have also been proposed, though this assumes that LV feeders never encounter technical issues [21] or that they are represented through approximated models, i.e., sensitivity factors and linearized flows [22].

In light of the above, some researchers believe that instead of investing in the P-Q chart approach, the community should resort to a proposal already well-established by several national grid operators: that distribution systems do not require such an advanced level of sophistication; it is sufficient to independently support higher voltage levels by ensuring their operation conforms to pre-decided technical standards [23]. Simply put, DS should be encouraged to minimally stress higher voltage levels and, whenever possible, to autonomously provide voltage support and some controllability on the drawn/injected active power [24], [25]. It is the authors' professional opinion that if all the LV feeders connected to the MV system behave in pre-approved, MV grid-friendly manner, i.e., minimal stress or/and provision of ancillary support, the DSO would have to invest less resources to combating technical issues, and could potentially sharpen its focus to building a more solid/reliable coordination framework with the TSO. Ideally, to allow for exact validation, one would have perfect knowledge and controllability of the MV-LV system [26], [27]. This would allow for a holistic approach to constraints management and AS provision. However, due to the inherent barriers (e.g., scalability, data trafficking, privacy), the authors resort to the more reliable approach of managing multi-feeder areas supplied by a single MV-LV substation.

This work adopts a novel, more "industrial" viewpoint in designing what the authors call the "LV to MV support framework" or LV2MV. The decision is motivated by a) the industry's need of a more reliable framework for evaluating the impact/support potential of LV networks on the MV grid (as compared to common simplified models, which are unreliable for highly active DS), and b) TSOs and DSOs are, in general, more willing to expand currently applied processes rather than implementing new ones [28]. The authors explore, for the first time, how more traditional HV-MV AS schemes, focusing on congestion and voltage support, could serve as inspirations for designing a practical MV-LV cooperation framework. The work is not solely concerned with conceptualization and rigorous mathematical (re)formulations, but also with a) ensuring that DSO and involved customers (SSBs) are sharing responsibilities, and b) designing a scalable and feasible methodology. By significantly extending our previous works [3], [29]

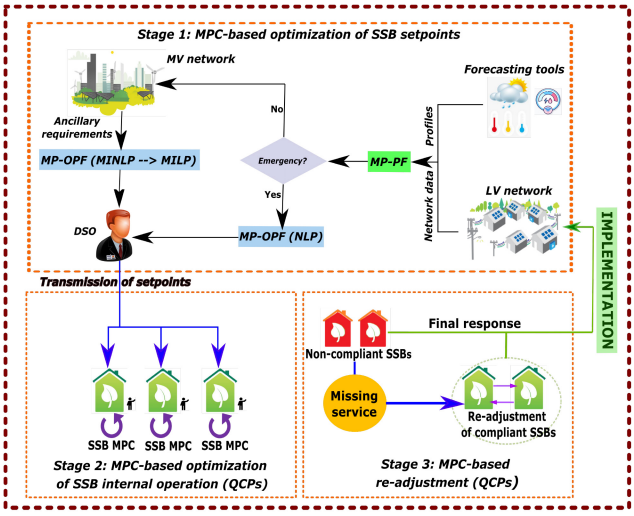

Fig. 1. Proposed 3-stage approach.

(scalability, detailed SSB models, conceptualization-rigorous formulation/reformulation of LV2MV AS, multiple customer types), this work offers the following major contributions.

- A novel, scalable, 3-stage, model predictive control (MPC)-based approach for the SSB-driven management of unbalanced LV feeders. It addresses network constraints management and AS provision from SSBs to the DSO, in the context of a MV-LV coordination framework, distributing responsibilities to DSO and SSBs.
- A first-time investigation of how classic AS schemes, designed in the framework of HV-MV coordination, could be adapted to LV networks. This work i) introduces detailed MINLP models of Swiss and Belgian AS schemes and their re-formulation to MILP equivalents, and ii) explores their behavior and impact in LV settings.
- Under the umbrella of "comprehensive performance assessment", this work includes a) a preliminary analysis of its robustness against communication failures, b) an investigation of the pros and cons of linearizations within the scope of the proposed approach, and c) a comparison to the approach's predecessor in [3].

Placing aside the technical novelty, a fundamental objective is to contribute, however much, to sparking the discussion and research initiative towards the development of novel and more sophisticated MV-LV cooperation frameworks. As such, this work should primarily be viewed under the lens of "new concept discussion and exploration".

II. Full Rundown of Proposed 3-Stage Approach

A. Main Idea

The DSO's *primary goal* is to prevent/mitigate any foreseen technical violation in the LV network, i.e., overvoltages, undervoltages, and line congestions. If, however, issue-free operation is expected, the DSO can, instead of remaining passive, resort to a *secondary goal*, and utilize its network's resources to provide ancillary services to the MV network. This way, there is always an incentive for the DSO to be actively involved in LV network management; in this work, this is realised through the 3-stage concept seen in Fig. 1.

At every time-step, the DSO runs a multi-period power flow (MP-PF) for a horizon length that has been deemed operationally acceptable/reliable. Do note that while any horizon length could be used in theory, it should be harmonized with the specific needs of the network or application in question, as well as with the device technical requirement of the SSBs.

If any of the 3 types of potential violations are expected to occur at any point within the horizon, the LV network enters into its emergency mode (Section II-B2), where all internal flexibility resources are exclusively dedicated to combating the aforementioned technical issues. If, however, none are reasonably foreseen, the LV network enters into its AS mode (Section II-B3), where the DSO instead utilizes its internal flexibility resources to provide ancillary support to the MV level (exact details are provided in Section II-B3).

Depending on the objective (emergency or AS mode), one of two different versions of a centralized MPC-driven multi-period optimal power flow (MP-OPF) establishes the ideal power profiles for all SSBs. Subsequently, said profiles are transmitted from the DSO to their respective recipients, in the form of non-binding profile modification requests (stage 1). After the requests have been submitted, the SSBs try to comply, while also optimizing any number of their own internal objectives at the same time (stage 2). Aside from compliance, the SSBs' main objective in this work is to minimize their sustainability deterioration, i.e., to maximize the injected active power from renewable generation (here PVs). After stage 2, the missing flexibility stemming from "non-compliant" SSBs is automatically assigned to originally "compliant" SSBs, following a tried-and-tested rule-based approach (stage 3) [3]. SSBs that can provide additional flexibility compensate for SSBs that have exhausted their own; the re-assignment process takes place instantly, without further involvement from the DSO.

The process repeats throughout the day for all 3 stages, taking into account updated forecasts (through MPC) at each time-step. For clarification, it should be stated that the building-based MPC does not explicitly model temperature control. Instead, all temperature-dependent devices (HVACs, heaters, etc.) are considered as part of the SSB's general flexible load (FL), or as part of the fixed load, fully controlled by the owner; this is a relatively common assumption [30].

B. Stage 1: LV Network Optimization by DSO

At each time-step, based on the forecasted and planned customer behavior, the DSO obtains an estimate of the network's state for a given look-ahead horizon. This may include technical violations (voltages, congestions) or/and negative impacts on the MV system, i.e., low power factors (*pf*) or undesirable reactive power contributions to the substation's voltage. Appropriate control actions must be planned in due time, as the controllable elements, here SSBs, cannot instantly react to large and rapid changes in the system, due to inherent ramping limitations. The use of MPC can surpass this hurdle by constantly "refreshing" the planned actions. The network is managed in two modes: normal and emergency.

1) LV Network Control Means: The DSO's tools for managing the system are its control requests towards SSBs. If one defines the short-term planned SSB behavior as $P^{\mathrm{F}}, Q^{\mathrm{F}}$, the requests $P^{\mathrm{R}}, Q^{\mathrm{R}}$ are defined in (1)-(2), where Δ^+, Δ^- stand for consumption increase, and decrease respectively. Ramping limitations are imposed on power requests (3)-(4):

$$P^{\mathrm{R}}_{\mathrm{i,t}} = P^{\mathrm{F}}_{\mathrm{i,t}} + \Delta P^{+}_{\mathrm{i,t}} - \Delta P^{-}_{\mathrm{i,t}} \tag{1}$$

$$Q^{\mathrm{R}}_{\mathrm{i,t}} = Q^{\mathrm{F}}_{\mathrm{i,t}} + \Delta Q^{+}_{\mathrm{i,t}} - \Delta Q^{-}_{\mathrm{i,t}} \tag{2}$$

$$\left|\Delta P^{+}_{\mathrm{i,t+1}} - \Delta P^{+}_{\mathrm{i,t}} - \Delta P^{-}_{\mathrm{i,t+1}} + \Delta P^{-}_{\mathrm{i,t}}\right| \leq R^{\mathrm{P,max}} \tag{3}$$

$$\left|\Delta Q^{+}_{\mathrm{i,t+1}} - \Delta Q^{+}_{\mathrm{i,t}} - \Delta Q^{-}_{\mathrm{i,t+1}} + \Delta Q^{-}_{\mathrm{i,t}}\right| \leq R^{\mathrm{Q,max}}. \tag{4}$$

2) LV Network Emergency Mode: If the system is foreseen to experience technical issues, i.e., overvoltages and undervoltages ($\sigma^{\mathrm{ov}}_{\mathrm{i,t}}, \sigma^{\mathrm{uv}}_{\mathrm{i,t}}$) or line congestions ($\sigma^{\mathrm{cg}}_{\mathrm{ij,t}}$), the DSO must minimize the issues (F_1, with violation cost C_1), with minimal customer disturbance (F_2, with request cost C_2):

$$\begin{aligned}\min(F_1 + F_2) = C_1 \cdot \sum_{\mathrm{t,i,j:i\neq j}} \left(\sigma^{\mathrm{ov}}_{\mathrm{i,t}} + \sigma^{\mathrm{uv}}_{\mathrm{i,t}} + \sigma^{\mathrm{cg}}_{\mathrm{ij,t}}\right) \\ + C_2 \cdot \sum_{\mathrm{t,i}} \left(\Delta P^{+}_{\mathrm{i,t}} + \Delta P^{-}_{\mathrm{i,t}} + \Delta Q^{+}_{\mathrm{i,t}} + \Delta Q^{-}_{\mathrm{i,t}}\right).\end{aligned} \tag{5}$$

3) LV Network Ancillary Service Mode: If, for the optimization horizon, the system is not expected to encounter technical violations, it enters into AS mode. The conservative assumption ensures no oscillation between operating modes within the optimization horizon. In making DS more active, the LV grid is envisioned to support the MV grid through some form of AS. While the concept sees wider application in the HV-MV interface [31], [32], the "smart grid vision" [33] is to expand it to the MV-LV interface. In this work, two AS schemes are adapted to the MV-LV interface: a) passive scheme (management of the substation's P-Q conditions), and b) active scheme (monitoring of the substation's pre-planned V-Q conditions). The described ancillary services are dedicated to the voltage control support of MV networks.

a) Passive schemes: limit the network's impact at the interface between voltage levels. This is achieved by imposing a minimum *pf* requirement, which depends on the active power intake. In some countries, e.g., Belgium, active power provision by distribution systems is a sought-after service; the *pf* limitation is less strict in cases of reverse power flows to higher voltage levels. The Belgian TSO defines three *pf*-based operation/penalization zones [31], see Fig. 2. Normally, the scheme is applied for entire distribution systems and on a yearly basis. Under the expectation of individual LV networks becoming self-managing, one can devise similar schemes for a single LV network and for the daily setting:

- Zone 1 ($\cos\phi \geq 0.95$ or $\tan\phi \leq 0.33$): the desirable, cost-free zone.
- Zone 2 ($\cos\phi \in [0.8, 0.95]$ or $\tan\phi \in [0.33, 0.77]$): a problematic zone, somewhat stressing the upper system. A penalty is applied per exchanged kVar (Q^{ex}).

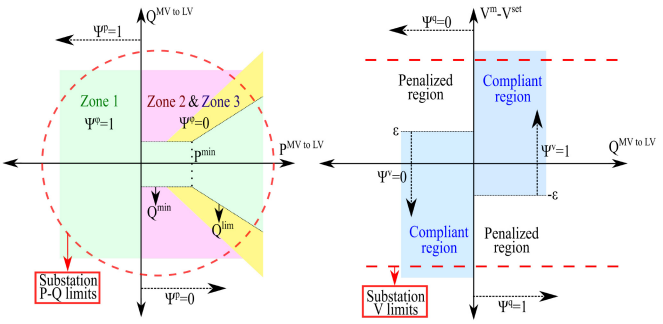

Fig. 2. Passive (left) and active (right) scheme. First is inspired by Belgian TSO's proposal of *pf*-based price zones [31]. Second is inspired by Swiss TSO's proposal of penalizing deviations from a pre-defined voltage profile [31] (fig. is illustrative, not drawn to scale).

- Zone 3 ($\cos\phi \leq 0.8$ or $\tan\phi \geq 0.77$): a highly problematic zone, requiring extensive reactive support. A high penalty is applied per exchanged kVar.

The passive objective is to minimize F_3^{pass}, described by (6). For simplicity, Zones 2, 3 are bundled together:

$$\min F_3^{\mathrm{pass}} = \begin{cases} C_3^{\mathrm{P}} \cdot \left(|Q^{\mathrm{ex}}| - Q^{\mathrm{lim}}\right), & \text{Zones 2, 3} \\ 0, & \text{Zone 1} \end{cases} \tag{6}$$

Objective F_3^{pass} is expressed in proper mixed-integer form as follows. First, the big-M parameter M^{p} and the binary variables $\Psi^{\mathrm{p}}, \Psi^{\phi}$ are defined: the first binary variable indicates whether active power is drawn from (0) or injected to (1) the MV system; the second one indicates if the exchanged reactive power is above (0) or below (1) the limit. Penalties are applied if Ψ^{p}=Ψ^{ϕ}=0. The passive objective F_3^{pass} is formulated as:

$$F_3^{\mathrm{pass}} = C_3^{\mathrm{P}} \cdot \left(1 - \min\{1, \Psi^{\mathrm{p}} + \Psi^{\phi}\}\right) \cdot \left(\left|Q^{\mathrm{ex}}\right| - Q^{\mathrm{lim}}\right) \tag{7}$$

$$-\Psi^{\mathrm{p}} \cdot M^{\mathrm{p}} \leq P^{\mathrm{ex}} \leq \left(1 - \Psi^{\mathrm{p}}\right) \cdot M^{\mathrm{p}} \tag{8}$$

$$M^{\mathrm{p}} \cdot \left(1 - \Psi^{\phi}\right) + \Psi^{\mathrm{p}} \cdot M^{\mathrm{p}} \geq \left|Q^{\mathrm{ex}}\right| - Q^{\mathrm{lim}} \geq -M^{\mathrm{p}} \cdot \Psi^{\phi} \tag{9}$$

$$Q^{\mathrm{lim}} = Q^{\mathrm{min}} + P^{\mathrm{ex}} \cdot \left(0.33 \cdot P^{\mathrm{min}} - Q^{\mathrm{min}}\right) / P^{\mathrm{min}}. \tag{10}$$

b) Active schemes: require the MV-LV interface to track a reference power or voltage profile, traditionally calculated during the day-ahead reactive power planning. In this work, the Swiss model is adopted, which tracks a voltage profile, V^{set} [26]. The network is compliant when its reactive energy exchange assists in tracking said profile, i.e., providing reactive power when the voltage, V^{m} is below V^{set}, and vice versa, see Fig. 2. A small deviation tolerance ϵ is allowed. When the network is compliant, it is remunerated (negative cost) based on the exchanged reactive power and vice versa.

The active objective is to minimize F_3^{act}, described by (11):

$$\min F_3^{\mathrm{act}} = \begin{cases} -C_3^{\checkmark} \cdot |Q^{\mathrm{ex}}|, & \text{if compliant} \\ C_3^{\mathrm{x}} \cdot |Q^{\mathrm{ex}}|, & \text{if non-compliant} \end{cases} \tag{11}$$

Objective F_3^{act} is expressed in proper mixed-integer form as follows. First, the big-M parameter M^{v} and the binary variables $\Psi^{\mathrm{q}}, \Psi^{\mathrm{v}}$ are defined: the first binary variable indicates if reactive power is drawn from (1) or injected to (0) the MV system; the second one indicates if the measured voltage is

above (1) or below (0) the set value. Ψ^{q}=Ψ^{v} translates to compliance. The active objective F_3^{act} is thus formulated as:

$$\begin{aligned}\min F_3^{\mathrm{act}} = &\left(-C_3^{\checkmark}\cdot\left|Q^{\mathrm{ex}}\right|\right)\\ &\cdot\left[\min\left\{\Psi^{\mathrm{q}},\Psi^{\mathrm{v}}\right\}+\left(1-\max\left\{\Psi^{\mathrm{q}},\Psi^{\mathrm{v}}\right\}\right)\right]+\left(C_3^{\mathrm{x}}\cdot\left|Q^{\mathrm{ex}}\right|\right)\\ &\cdot\left(\max\left\{\Psi^{\mathrm{q}},\Psi^{\mathrm{v}}\right\}-\min\left\{\Psi^{\mathrm{q}},\Psi^{\mathrm{v}}\right\}\right) \quad (12)\end{aligned}$$

$$M^{\mathrm{v}}\cdot\Psi^{\mathrm{q}} \geq Q^{\mathrm{ex}} \geq -M^{\mathrm{v}}\cdot\left(1-\Psi^{\mathrm{q}}\right) \quad (13)$$

$$-M^{\mathrm{v}}\cdot\left(1-\Psi^{\mathrm{v}}\right)+V^{\mathrm{set}}-\epsilon \leq V^{\mathrm{m}} \leq M^{\mathrm{v}}\cdot\Psi^{\mathrm{v}}+V^{\mathrm{set}}+\epsilon \quad (14)$$

Both objectives are computationally cumbersome, due to the bilinear terms and *abs*, min, max operators. This challenge is overcome by reformulating or approximating them to mixed-integer linear forms. Details are elaborated in the Appendix.

In general, active schemes are harder to reliably implement [26]. In some countries, they are remunerated when the compliance rate is consistently high; otherwise, the network reverts to a passive scheme (monthly evaluations) [26]. This work focuses on real-time optimization, so longer-term phenomena are out of scope. Even though it is defined mathematically, compliance is not evaluated outside the substation's limits (Fig. 2), as emergency mode would "kick in" in such cases.

C. Stage 2: Internal SSBs Optimization

The DSO may request SSBs to alter their aggregate power profile; the DSO has no information on the devices that the SSB hosts, nor on their phase distribution. Consequently, some of the responsibility is transferred to the SSB. The SSB should also keep the curtailment of its on-site renewable production to a minimum (to avoid compromising its nZE status). Each SSB must thus minimize a) photovoltaic (PV) production curtailment[1] (F_4, with curtailment cost C_4), b) deviations from the DSO's requests (F_5, with deviation cost C_5), and c) imbalances between phases (F_6, with imbalance cost C_6). In the following, the superscripts *tot* and *avg* correspond to total SSB power and to average per-phase SSB power:

$$\min F^{\mathrm{SSB}} = F_4+F_5+F_6 \quad (15)$$

$$F_4 = C_4\cdot\sum_t\left(S_{\mathrm{b,t}}^{\mathrm{gen}}-P_{\mathrm{b,t}}^{\mathrm{inj}}\right) \quad (16)$$

$$F_5 = C_5\cdot\sum_{\mathrm{t}}\left[\left(P_{\mathrm{b,t}}^{\mathrm{R}}-P_{\mathrm{b,t}}^{\mathrm{tot}}\right)^2+\left(Q_{\mathrm{b,t}}^{\mathrm{R}}-Q_{\mathrm{b,t}}^{\mathrm{tot}}\right)^2\right] \quad (17)$$

$$P_{\mathrm{b,t}}^{\mathrm{tot}} = \sum_{\mathrm{z}}P_{\mathrm{b,t,z}} \quad \& \quad Q_{\mathrm{b,t}}^{\mathrm{tot}} = \sum_{\mathrm{z}}Q_{\mathrm{b,t,z}} \quad (18)$$

$$F_6 = C_6\cdot\sum_{t,z}\left[\left(P_{\mathrm{b,t,z}}-P_{\mathrm{b,t}}^{\mathrm{avg}}\right)^2+\left(Q_{\mathrm{b,t,z}}-Q_{\mathrm{b,z,t}}^{\mathrm{avg}}\right)^2\right] \quad (19)$$

$$P_{\mathrm{b,t}}^{\mathrm{avg}} = P_{\mathrm{b,t}}^{\mathrm{tot}}/3 \quad \& \quad Q_{\mathrm{b,t}}^{\mathrm{avg}} = Q_{\mathrm{b,t}}^{\mathrm{tot}}/3. \quad (20)$$

D. Stage 3: Missing Service Mitigation

Some SSBs may be unable to adequately comply with the DSO's request. Ideally, the DSO would re-run the optimization and send renewed signals to the remaining SSBs. However, this could involve multiple MP-OPFs, which is impractical for online processes. In that light, each *originally compliant* SSB immediately receives a re-adjustment signal according to its original flexibility contributions.

SSB are either compliant (*CB*) or non-compliant (*NCB*). The total active/reactive non-compliance is defined, i.e., the total requested flexibility amount that is not delivered, as $NC_{\mathrm{t}}^{\mathrm{P/Q}}$ (21)-(22), and the extra effort for a compliant SSB, i.e., the additional flexibility amount that it is asked to provide, as $AE_{b\in CB,t}^{\mathrm{P/Q}}$ (23)-(24). The process is repeated until all requests are met or until SSBs can provide no further support:

$$NC_{\mathrm{t}}^{\mathrm{P}} = \sum_{b\in NCB}\Delta P_{\mathrm{b,t}}^{\mathrm{real}} \quad \& \quad NC_{\mathrm{z,t}}^{\mathrm{Q}} = \sum_{b\in NCB}\Delta Q_{\mathrm{b,t}}^{\mathrm{real}} \quad (21)$$

$$\Delta P_{\mathrm{b,t}}^{\mathrm{real}} = P_{\mathrm{b,t}}^{R}-P_{\mathrm{b,t}}^{\mathrm{actual}} \quad \& \quad \Delta Q_{\mathrm{b,t}}^{\mathrm{real}} = Q_{\mathrm{b,t}}^{R}-Q_{\mathrm{b,t}}^{\mathrm{actual}} \quad (22)$$

$$AE_{b\in CB,t}^{\mathrm{P}} = NC_{\mathrm{t}}^{\mathrm{P}}\cdot\left(1-\frac{\left|P_{\mathrm{b,t}}^{R}-P_{\mathrm{b,t}}^{F}\right|}{\sum_{b\in CB}\left|P_{\mathrm{b,t}}^{R}-P_{\mathrm{b,t}}^{F}\right|}\right) \quad (23)$$

$$AE_{b\in CB,t}^{\mathrm{Q}} = NC_{\mathrm{t}}^{\mathrm{Q}}\cdot\left(1-\frac{\left|Q_{\mathrm{b,t}}^{R}-Q_{\mathrm{b,t}}^{F}\right|}{\sum_{b\in CB}\left|Q_{\mathrm{b,t}}^{R}-Q_{\mathrm{b,t}}^{F}\right|}\right). \quad (24)$$

III. Network and Building Modeling

The DSO and SSBs are each concerned with managing their own system. The employed models are hereby described.

A. Stage 1 (DSO Side): LV Feeder-Level Modeling

1) Electrical Network: LV feeders are generally unbalanced. Ideally, the DSO would send SSBs per-phase requests [3], [29]. However, this requires technical infrastructure that is perhaps too sophisticated. In this work, the DSO's optimization is based on the 1-phase (1Φ) equivalent. To validate whether imbalances are sufficiently mitigated at the SSB level (F_6), a final check is performed on the 3Φ equivalent.

Contrary to [3], the use of voltage rectangular coordinates is not well-suited for the examined problem, mainly due to having to decouple state and control variables (to allow for proper monitoring at the substation). This work employs polar coordinates, the terms P_{ij}, Q_{ij} and θ_{ij} representing active/reactive power flows and nodal angular differences, respectively. The model also includes active and reactive[2] power balances (25) and power flows (26)-(27), and network technical limits, i.e., upper/lower voltage magnitudes, $V^{\max}$, $V^{\min}$, and branch flow maximum apparent power, $S_{\mathrm{ij}}^{\max}$, (28)-(29). For (28)-(29), the slack variables are assumed as zero in AS mode (see Fig. 1). The constraints hold $\forall i,j\in\mathcal{I}: i\neq j, \forall t\in\mathcal{T}$:

$$P_{\mathrm{i,t}}^{\mathrm{R}}+P_{\mathrm{i,t}}^{\mathrm{fixed}} = \sum P_{\mathrm{ij,t}} \ \& \ Q_{\mathrm{i,t}}^{\mathrm{R}}+Q_{\mathrm{i,t}}^{\mathrm{fixed}} = \sum Q_{\mathrm{ij,t}} \quad (25)$$

$$P_{\mathrm{ij,t}} = V_{\mathrm{i,t}}^2 g_{\mathrm{ij}}+V_{\mathrm{i,t}}V_{\mathrm{j,t}}\left(-g_{\mathrm{ij}}\cos\theta_{\mathrm{ij,t}}-b_{\mathrm{ij}}\sin\theta_{\mathrm{ij,t}}\right) \quad (26)$$

$$Q_{\mathrm{ij,t}} = -V_{\mathrm{i,t}}^2 b_{\mathrm{ij}}+V_{\mathrm{i,t}}V_{\mathrm{j,t}}\left(-g_{\mathrm{ij}}\sin\theta_{\mathrm{ij,t}}+b_{\mathrm{ij}}\cos\theta_{\mathrm{ij,t}}\right) \quad (27)$$

[1] $S_{\mathrm{b,t}}^{\mathrm{gen}}$ is used to signify penalization because of curtailment AND because of conversion to reactive power.

[2] Note that at the substation, $P_{\mathrm{ij,t}}, Q_{\mathrm{ij,t}}$ correspond to $P_{\mathrm{t}}^{\mathrm{ex}}, Q_{\mathrm{t}}^{\mathrm{ex}}$.

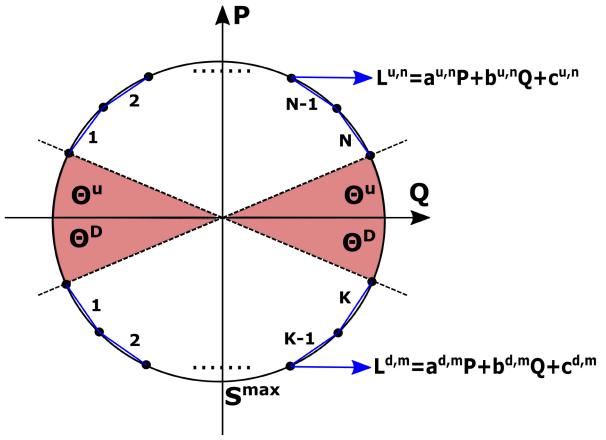

Fig. 3. Piecewise linearization of power flow limit (29).

$$V^{\min} - \sigma^{\text{uv}}_{\text{i,t}} \le V_{\text{i,t}} \le V^{\max} + \sigma^{\text{ov}}_{\text{i,t}} \tag{28}$$

$$\left(P_{\text{ij,t}}\right)^2 + \left(Q_{\text{ij,t}}\right)^2 \le \left(S^{\max}_{\text{ij}}\right)^2 + \sigma^{\text{cg}}_{\text{ij,t}}. \tag{29}$$

2) Examined Problem and Approximations: The network optimization (stage 1) involves two sub-problems; only one is solved per time-step, depending on the foreseen system state, previously determined by a MP-PF. Both contain the network equations and constraints (25)-(29), and the objective F_2. The emergency sub-problem concerns objective F_1 and is NLP, while the AS sub-problem concerns one of the objectives F_3^{pass}, F_3^{act} and is MINLP. The latter is, in general, intractable.

To overcome the intractability, a mixed-integer linear (MILP) approximation is proposed, which can be comfortably handled by commercial solvers. The linearizations concern the power flow equations (26)-(27) and limits (29). The goal is to showcase the proposed methodology for incorporating AS schemes; the employed linearization is generic, and *not necessarily* tailored to the specific needs of the problem.

For the power flows (26)-(27), assuming estimated values for voltages and power angles, i.e., $\iota^* = \{V^*_{\text{i,t}}, V^*_{\text{j,t}}, \theta^*_{\text{ij,t}}\}$, see [34], [35], a first-order Taylor series expansion is employed (30)-(31). The impact that the selection of ι^* has on the approximation's accuracy will be explored in the results section:

$$P_{\text{ij,t}} \approx P^*_{\text{ij,t}} + \left(\iota - \iota^*\right)\left[\frac{\partial P_{\text{ij,t}}}{\partial V_{\text{i,t}}}\Big|_{\iota^*} \quad \frac{\partial P_{\text{ij,t}}}{\partial V_{\text{j,t}}}\Big|_{\iota^*} \quad \frac{\partial P_{\text{ij,t}}}{\partial \theta_{\text{ij,t}}}\Big|_{\iota^*}\right]^{-1} \tag{30}$$

$$Q_{\text{ij,t}} \approx Q^*_{\text{ij,t}} + \left(\iota - \iota^*\right)\left[\frac{\partial Q_{\text{ij,t}}}{\partial V_{\text{i,t}}}\Big|_{\iota^*} \quad \frac{\partial Q_{\text{ij,t}}}{\partial V_{\text{j,t}}}\Big|_{\iota^*} \quad \frac{\partial Q_{\text{ij,t}}}{\partial \theta_{\text{ij,t}}}\Big|_{\iota^*}\right]^{-1} \tag{31}$$

For the branch flow limit (29), a version of the piecewise linearization presented in [34] is employed. The attention now shifts to the apparent power flow constraint cycle, see Fig. 3. The angles Θ^u, Θ^d are defined, which delineate the feasible area where the power flow is rarely located, and K, N (number of linear equidistant segments used to approximate the quadratic constraint). The constraint (29) can be approximated by the set of $K + N$ linear constraints (32), where the a, b, c are separately calculated for each linear segment ($n \in \{1, \ldots, N\}, k \in \{1, \ldots, K\}$).

$$(29) \rightarrow \begin{cases} L^{\text{u,n}}_{\text{ij}} = a^{\text{u,n}} \cdot P_{\text{ij}} + b^{\text{u,n}} \cdot Q_{\text{ij}} + c^{\text{u,n}} \ge 0 \\ L^{\text{d,k}}_{\text{ij}} = a^{\text{d,k}} \cdot P_{\text{ij}} + b^{\text{d,k}} \cdot Q_{\text{ij}} + c^{\text{d,k}} \ge 0. \end{cases} \tag{32}$$

B. Stages 2 & 3 (SSB Side): Device Modeling

SSBs may host various devices, such as flexible loads (FLs), renewables (PVs) and low-carbon technologies (here electric vehicles-EVs). As is common, it is assumed that all 3 phases host controllable loads (non-uniform distribution). While the norm is to see PVs and EVs as single-phase connections, the deployment of the (more expensive) 3Φ inverter configuration has gained traction, due to its ability for reducing operational costs for building owners and the network [29]. All constraints hold $\forall z \in \mathcal{Z},\ \forall p \in \mathcal{P},\ \forall e \in \mathcal{E},\ \forall b \in \mathcal{B},\ \forall f \in \mathcal{F}$.

1) Photovoltaics: For 1Φ PVs, the apparent generated power, $S^{\text{gen}}_{\text{p,t}}$, can be curtailed up to Ω^{PV} (33), resulting into the inverter-level apparent power, $S^{\text{inv}}_{\text{p,t}}$. The PV's flexible *pf* also allows for the utilization of reactive power, said flexibility being limited by a relaxed production capability curve (34)-(35), where Ω^{Q} denotes the maximum percentage of apparent power that can be converted to reactive power. For 3Φ PVs, the power output can be distributed among the three phases [36]. The total, 3Φ active power injection *must be equal* to the original 1Φ injection (36). The re-distribution limit depends on the rate of each 1Φ inverter, $P^{\text{rate}}_{\text{p}}$, (37). *Individual* inverters may consume active power, an especially useful capability during nighttime (zero PV production [36]):

$$S^{\text{gen}}_{\text{p,t}}\left(1 - \Omega^{\text{PV}}\right) \le S^{\text{inv}}_{\text{p,t}} \le S^{\text{gen}}_{\text{p,t}} \tag{33}$$

$$\left(Q^{\text{inj}}_{\text{p,t}}\right)^2 + \left(P^{\text{inj}}_{\text{p,t}}\right)^2 \le \left(S^{\text{inv}}_{\text{p,t}}\right)^2 \tag{34}$$

$$-\Omega^{\text{Q}} \cdot S^{\text{inv}}_{\text{p,t}} \le Q^{\text{inj}}_{\text{p,t}} \le \Omega^{\text{Q}} \cdot S^{\text{inv}}_{\text{p,t}} \tag{35}$$

$$\text{If } 3\Phi: \quad \sum_{z} P^{\text{inj}}_{\text{p,z,t}} = P^{\text{inj}}_{\text{p,t}} \tag{36}$$

$$\text{If } 3\Phi: \quad -P^{\text{rate}}_{\text{p}}/3 \le P^{\text{inj}}_{\text{p,z,t}} \le P^{\text{rate}}_{\text{p}}/3. \tag{37}$$

2) Electric Vehicles: Traditional (charge-only) 1Φ EVs can charge more or less, $P^{\text{change}}_{\text{e,t}}$, than originally planned, $P^0_{\text{e,t}}$ [29]. EVs cannot charge while absent from a building's premises, denoted by time sub-set $\mathcal{T}^{nc}_e$ (38). Net changes across the optimization horizon should be zero (39), and technically feasible (40). EVs are assumed to operate with a unity *pf*. For 3Φ EVs, (36)-(37) are adapted as (41)-(42):

$$P^{\text{change}}_{\text{e,t}} = 0 \quad \forall t \in \mathcal{T}^{nc}_e \tag{38}$$

$$\sum_{\text{t}}\left(P^{\text{change}}_{\text{e,t}}\right) = 0 \tag{39}$$

$$0 \le P^0_{\text{e,t}} + P^{\text{change}}_{\text{e,t}} \le P^{\text{rate}}_{\text{e}} \tag{40}$$

$$\sum_{\text{z}} P^0_{\text{e,z,t}} + P^{\text{change}}_{\text{e,z,t}} = P^0_{\text{e,t}} + P^{\text{change}}_{\text{e,t}} \tag{41}$$

$$-1/3 \cdot P^{\text{rate}}_{\text{e}} \le P^0_{\text{e,z,t}} + P^{\text{change}}_{\text{e,z,t}} \le 1/3 \cdot P^{\text{rate}}_{\text{e}}. \tag{42}$$

3) Flexible Loads: For FLs like controllable house appliances (constant-P model), the active power, $P_{\text{f,z,t}}$ may be altered up to Ω^{FL} (43). Within the optimization horizon, net changes with respect to the original FL profile, $P^{\text{original}}_{\text{f,z,t}}$, must be zero (44). A fixed *pf* of 0.95 is assumed for all FLs:

$$P_{\text{f,z,t}} \cdot \left(1 - \Omega^{\text{FL}}\right) \le P_{\text{f,z,t}} \le P_{\text{f,z,t}} \cdot \left(1 + \Omega^{\text{FL}}\right) \tag{43}$$

$$\sum_{\text{t}}\left(P_{\text{f,z,t}} - P^{\text{original}}_{\text{f,z,t}}\right) = 0. \tag{44}$$

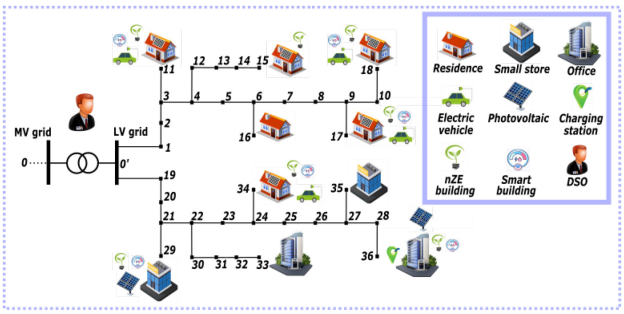

Fig. 4. Examined two-feeder LV network.

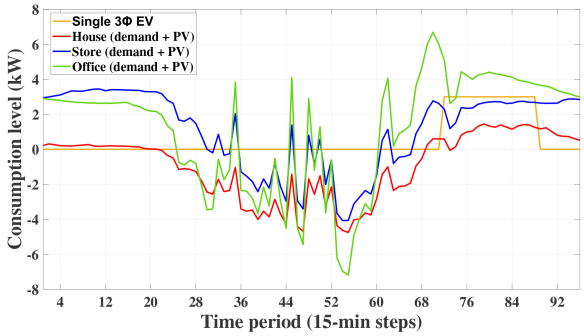

Fig. 5. Initially forecasted building & device profiles.

4) Examined Problem: The SSB optimization problem (stage 2, with possible input from stage 3) comprises the quadratic building objective (15) and the various device models (33)-(44). All constraints are linear, except for quadratic PV constraint (34). The SSB quadratically-constrained (QCP) problem can be comfortably handled by commercial solvers.

IV. Case Study

A. Simulation Environment

The proposed approach is applied on a two-feeder LV network, comprising a residential area of 2-4 person households and a commercial area of small stores (e.g., boulangeries) and offices (e.g., public administration buildings), see Fig. 4. Both feeders are modified versions of the 18-node CIGRE LV feeder [37]. Most buildings are smart, i.e., can receive requests and control their FLs, PVs and EVs (if such devices are hosted). The commercial area also hosts a charging station, serving none to all available EVs (random). The typical, 24-hour profile of each building (positive-consumption, negative-production) is depicted in Fig. 5. The data is fully representative, and is provided by Luxembourg's TSO/DSO, CREOS [38], [39]. Additional information pertaining to the case study is available in Tables I, II. All financial parameters are chosen in order to simulate the *desired prioritization or behavior* from each entity in the scope of the optimization, without necessarily corresponding to real-life values [29]. Naturally, when expanding this work, one may choose alternative values.

For each building, the consumption or production forecast for all devices (except EVs) is updated at each time-step (15-min steps considered) to account for the flow of new information on the weather and on the consumption needs. Similarly to [3], it is assumed that the forecasting deviation is linearly dependent on the distance from the current time-step, varying between 1% (first time-step) and 20% (last time-step). PVs and EVs are assumed to be 3Φ, while FLs are connected to one, two, or three phases (random selection).

Simulations are performed in GAMS, on a PC of 2.7-GHz and 8-GB RAM, using the solvers IPOPT (NLP), CPLEX (MILP), and BONMIN (MINLP) with default settings.

TABLE I
Characteristics/Costs for Buildings

Parameter	House	Store	Office
PV rated power (kW)	5	7	14
EV rated power (kW)	3	–	–
Installed load (kW)	15	30	50
Power factor (pf)	0.95	0.95	0.9
Ramp rate $R^{\text{P,max}}$ (kW/15min)	1	2	3
Ramp rate $R^{\text{Q,max}}$ (kVar/15min)	0.1	0.2	0.3
No charging period $\mathcal{T}_e^{nc}$	09.00-18.00	–	17.00-10.00
Curtailment capability Ω^{PV}	0.3	0.5	0.8
Reactive power capability Ω^{Q}	0.2	0.3	0.5
Load flexibility Ω^{FL}	0.4	0.3	0.2
Curtailment cost C_4 (€/kW)	20	25	30
Non-compliance cost C_5 (€/kW^2)	5	7	10
Imbalance cost C_6 (€/kW^2)	3	5	10
Device 3Φ distribution (a-b-c, %)	32-38-30	35-28-37	29-34-37

TABLE II
Characteristics/Costs for Grid and Ancillary Schemes

Parameter	Value	Concerns the...
$P^{\min}$ (kW)	$0.5 \cdot P^{\text{peak}}$	passive scheme
$Q^{\min}$ (kVar)	$0.33 \cdot P^{\min}$	passive scheme
Penalty in zones 2, 3 C_3^{p} (€/kVar)	5	passive scheme
Compliance reward $C_3^{\checkmark}$ (€/kVar)	3	active scheme
Non-compliance penalty C_3^{x} (€/kVar)	5	active scheme
Desired substation voltage V^{set} (p.u.)	1	active scheme
Voltage tolerance ϵ (p.u.)	0.02	active scheme
Violations cost C_1 (€/p.u.)	100	grid operator
Request cost C_2 (€/kW or €/kVar)	2	grid operator

TABLE III
Daily Network Costs (24 Hours, 6-Hour Horizon)

	MINLP		MILP		Original
	w/o Stage 3	w. Stage 3	w/o Stage 3	w. Stage 3	
Violation costs (€)	17.2	0.7	17.1	0.7	175
Passive penalties (€)	12.4	0	12.5	0	47.2
Active penalties (€)	-18.3	-56.1	-17.6	-55.06	32.6
Request costs (€)	82.5	39.3	83.9	39.7	–
Total solution time* (s)	20,102.6	20,318.9	984.2	1,193.7	–

*Refers to (stage 1 + stage 2 + stage 3) summed over all 96 iterations

B. Behavior of Ancillary Services Schemes

First, the performance of the proposed AS schemes (see Section II-B2) is investigated. Table III presents the daily network-related costs, with and without any optimization, with and without stage 3 (re-adjustment), for a look-ahead horizon of 24 15-min periods (6 hours), a solid choice as it pertains to granularity-solution time trade-off [3]. When the DER-heavy network is left uncontrolled (original), it clearly cannot support any AS scheme (high passive and active costs); it also experiences high violation costs (175 €, i.e., 1.75 p.u. daily cumulative voltage and line violations). Under the proposed approach, the DSO employs targeted customer requests to

TABLE IV
ANCILLARY SCHEMES SENSITIVITY ANALYSIS (24 HOURS, 6-HOUR HORIZON, MILP FORMULATION)

Active		Passive	
Sensitivity ϵ	Total daily cost (€)	Power factor limit	Total daily cost (€)
0.05	-98.7	0.90	11.4
0.02 (Swiss)	-55.06	0.95 (Belgian)	40.0
0.01	-10.8	0.98	69.7
0.00 (Extreme)	30.4	1.00 (Extreme)	104.1

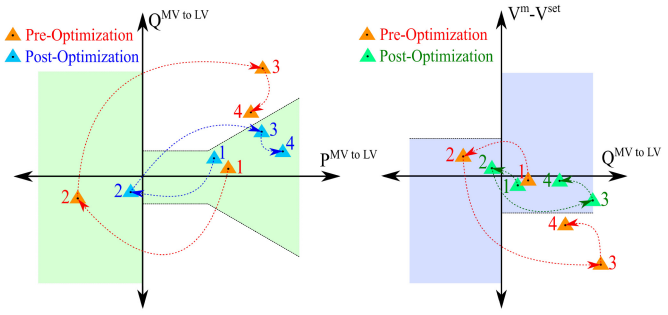

Fig. 6. Performance of ancillary schemes in characteristic hours (left-passive, right-active).

TABLE V
PERFORMANCE PER LOOK-AHEAD HORIZON (ITERATION) AND STAGE

Stage and solution time (s)	Look-ahead horizon (periods/hours) 2/0.5	4/1	12/3	24/6	96/24	24/24*
Stage 1 - Emergency (NLP)	0.55	0.73	2.08	5.46	12.95	4.87
Stage 2 - SSBs (QCPs)	0.20	0.31	0.83	1.75	2.78	1.69
Stage 3 - SSBs (QCPs)	0.22	0.46	0.97	1.64	2.91	1.81
Stage 1 - Passive (MILP)	0.49	0.71	1.24	2.47	4.07	3.02
Stage 1 - Active (MILP)	1.67	2.08	5.49	8.23	19.11	10.05
Stage 1 - Passive (MINLP)	5.71	10.11	49.12	103.32	673.1	92.54
Stage 1 - Active (MINLP)	12.06	20.63	98.83	182.74	1094.7	188.38
Passive mismatch (%)	6.01	3.87	1.79	1.36	1.30	3.31
Active mismatch (%)	5.72	3.57	1.66	1.25	1.26	5.49

*Special case: hourly time-step

TABLE VI
AS-ONLY LINEARIZATION PERFORMANCE (PASSIVE SCHEME)

Flow linearization (a)		Apparent flow limit linearization (b)	
ι^*	Mismatch (%)	K, N	Mismatch (%)
AC PF (used)	1.36	20 (used)	1.36
DC PF	6.03	15	1.78
Flat values	3.88	10	2.09
Random in limits	8.42	5	2.73

nearly eliminate all technical issues (99.6% reduction), ensure perfect application of the passive scheme (zero penalization) and maximize the voltage compliance in the stricter active scheme. System costs are reduced by 90.1% and 100% for the passive and active scheme, respectively (active scheme results in DSO profit). The differences between the MINLP, MILP problems lie at 1.36% (passive) and 1.25% (active).

The importance of stage 3 should also not be understated. SSB are at times unable to provide the requested flexibility, leading to larger requests and more violations (technical and ancillary-related), see Table III. The additional effort from "compliant" SSBs, despite not always being activated, has a noticeable impact on the cumulative cost profile of the network, as one can see if they add up all costs in Table III.

A sensitivity analysis of the proposed schemes is presented in Table IV, where different values of voltage sensitivity tolerance ϵ (active scheme) and power factor limit (passive scheme) are examined, other that those commonly proposed by TSOs for similar AS schemes. One can thus explore the range within which such schemes are well-suited for LV networks, and at which point they become non-viable. Naturally, relaxing the network's ancillary requirements translates to fewer customer requests, resulting in significant cost reductions. However, a single LV network cannot be expected to reliably maintain technically challenging conditions at the substation; its design is not compatible with extreme requirements and the resources are scarce. For instance, when the limits for ϵ and the *pf* are set to 0.01 and 0.98, respectively, network costs increase by 83% (active) and 148% (passive). Great care must thus be taken when designing similar ancillary schemes for LV networks.

Visualizing the behavior of the AS can reveal interesting information about their suitability and effectiveness. This behavior is presented in Fig. 6, which shows 4 characteristic hours, pre- and post-optimization, as well as the various transitions between them: late night (1), midday (2), when the highest levels of solar irradiation are observed, afternoon (3), when total building demand is at its highest, and early night (4), when EV charging is normally most intensive. Under normal conditions, the network "oscillates" within broad limits, with the substation experiencing drastic changes on its *pf* and voltage. The excessive reactive power consumption "drags" the *pf* below 0.95 and the voltage below the 0.98 p.u. desirable limit. Contrariwise, when SSBs are coordinated (given a sufficient look-ahead horizon), the network is compliant the vast majority of the time, and its various operating conditions are actually much tighter. Essentially, the substation's voltage and *pf* remain in stabler operation regions; the network is thus better primed for any potential unforeseen changes.

C. Computational Characteristics and Performance

A strong aspect of the proposed approach is that it can be scalable while sacrificing little accuracy at the optimal solution. This is a result of the linearizations *only being employed during AS mode*, i.e., when the system is not expected to be stressed, so any lost information at the limit has minimal impact on the solution (do however note that the above statements only hold for when the linerization's two main elements, i.e., vector ι^* and number of linear segments, K, N are properly selected, otherwise the drop in accuracy may be non-negligible, see Table VI). While indications were observed in Table III, this claim is further validated across all modes and stages, as well as for different look-ahead horizons, see Table V (note that SSBs and DSO share the same horizon length). Hereby, the term "mismatch" refers to the difference between the MINLP and MILP objective functions.

Even for the longest horizon, emergency stage 1, and stages 2, 3 solve very fast, together clocking in at 18.64s (2% of the 15-min time-step). The linearized ancillary stage 1 also solves reliably fast (2.47s for passive, 8.23s for active). Sacrificing only limited information for the MILP problem, the solution accuracy is impressive; the average mismatch in objective functions is 1.3% (6-hour horizon). Naturally, shorter horizons

improve the solution time, but at the expense of accuracy (MINLP-MILP) and, of course, of much higher network costs, see also [3]. The MINLP model (used for the sake of accuracy comparison) clocks in at 2-3 minutes, a reasonable, yet substantial chunk of the 15-min time-step. However, there is no guarantee that this observation would repeat for larger or more complex problems; in fact, when employing a 96-period horizon, a popular choice in look-ahead network applications, MINLP is unreliably slow. On average, it requires between 10 and 18 minutes, meaning it is clearly not viable for the chosen 15-min granularity.

One should bear in mind the importance of horizon and granularity selection: too broad look-ahead horizons, e.g., 24 hours, needlessly increase the solution time for minimal gains. Similarly, hourly time-steps (instead of 15-min) fail to accurately capture the profile of each building, which translates to much more drastic fluctuations in their behavior. This increases the flexibility and violation costs, giving a worse view of the network's conditions than is actually the case.

Exploring the linearization's performance adds further value to the work, hence the inclusion of Table VI. As is evident, while the number of linear segments in the flow limit does affect the solution accuracy, the effect is somewhat limited. Because the linearization takes place under lightly loaded conditions, the information lost at the flow limit has a limited impact on the solution. Using too few segments drastically changes the nature of the power flow, hence the noticeable deterioration of the objective function.

While not shown, fewer segments result in smaller problem size, i.e., faster solution speed. However, the solution is already fast enough to not warrant further speed-up at the moment. On the other hand, the estimated voltage/angle values must be carefully selected. This input can provide the DSO with a false sense of security or insecurity, resulting in unnecessary or insufficient customer requests, hence the erratic behavior of the objective function. For example, when using random inputs, i.e., simulating bad state estimation, the MILP problem returns a worse solution by more than 8%.

While fine-tuning the linearization is important, in this work, the authors went with a purposefully conservative set of inputs, since there was no a-priori guarantee for its performance. Said inputs remained the favourable choices following trial-and-error tests, with different numbers of linear segments K, N, and different estimation methods for the voltage-angle vector ι^*, see Table VI. Naturally, "tighter" inputs would presumably lead to increased accuracy, until a certain saturation point would be reached. However, since the linearization is not the paper's main focus, Table VI aims to draw attention to the dangers of carelessly converting problems from MINLP to MILP. Fully mitigating said dangers is not within paper scope.

D. Behavior of SSBs

SSBs constitute dominant players in the approach, so it makes sense to examine their internal operation. An example of how the proposed approach shapes a house's (node 17) daily operation is presented in Fig. 7. The differences are instantly noticeable. Aside from the fact that the consumption of typical loads is better distributed across the day, the PV and EV utilize their 3Φ inverters to balance out not only their own profiles, but also *any phase mismatches stemming from the loads*. Do also observe that PVs need to offer only limited reactive support, mostly in the afternoon, where larger SSBs have a high net load, causing the network to request increased reactive power injection. However, the most important observation is the fact that PVs and EVs, normally the main "troublemakers" in unbalanced systems, spread out their profile across the 3 phases very evenly. They thus prove themselves as useful tools when it comes to addressing multi-phase network issues without the DSO having to *directly address them.*

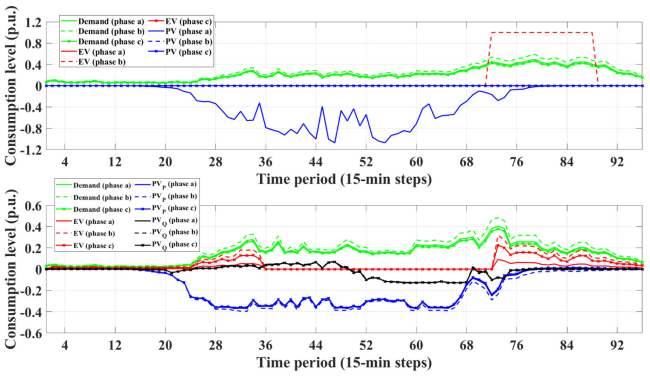

Fig. 7. Daily SSB device profiles pre-optimization (up) and post-optimization (down) for house at node 17.

The next target is to examine the cost allocation of SSBs with respect to the nZE directive and the received 1Φ requests. The active power of PVs is almost fully utilized (about 3.5% of total production is either curtailed or converted to reactive power), while there is practically no phase imbalance (about 1% of SSB costs are attributed to imbalance penalties). The largest percentage of SSB costs stems from non-compliance (more than 95% on average). This is a result of the 1Φ-3Φ modeling mismatch, and of the SSBs often running out of flexibility. However, the non-compliance is addressed with a high success rate through the automatic, coordinated re-adjustment; although not explicitly shown, more than 85% of all building flexibility requests are satisfied. It is also worth noting that all 3 building types provide similar normalized flexibility amounts, meaning no customer type dominates the network management process *when adjusting for size*.

E. Comparison With Predecessor

A natural next step is to compare the proposed approach to its predecessor, i.e., the idealized 3-stage approach of [3], where the DSO can make direct 3Φ power requests. The comparison is done in terms of cost and solution time, across all 3 stages; results are presented in Table VII. They concern solely the emergency management module, since the original 3-stage approach of [3] *did not grant the network* the opportunity to provide AS to the MV level.

The proposed approach results in slightly higher costs at network and building level (∼5% difference). Due to using the 1Φ equivalent, i.e., ignoring the per-phase aspect of the

TABLE VII
PERFORMANCE COMPARISON: NOVEL VS ESTABLISHED

Process	Novel		Established	
	Daily cost (€)	Sol. time (s)	Daily cost (€)	Sol. time (s)
Stage 1 (NLP)	27.10	5.46	25.4	42.5
Stage 2 (QCPs)	56.72	1.75	54.33	1.54
Stage 3 (QCPs)	18.12	1.64	14.29	1.39

TABLE VIII
PERFORMANCE FOR VARIOUS REQUEST FAILURE PROBABILITIES (MILP FORMULATION, 24 HOURS, 6-HOUR HORIZON)

Probability of request failure (%)	Total failures recorded (-)	Cost increase-passive scheme (%)	Cost increase-active scheme (%)
0	0	0 (benchmark)	0 (benchmark)
1	3	0.00	0.01
2	10	0.05	0.03
5	23	0.19	0.26
10	54	0.68	0.87

problem, the DSO requests more flexibility than is really needed. SSBs in turn opt for internal phase balancing instead of straightforward request compliance. After running the 3Φ PF (after stage 3), and subtracting non-compliance penalties from request costs, the final costs of each stage are finally calculated (in Table VII), which are nigh-identical for the two approaches. However, the novel one is actually 81% faster per optimized horizon. This leads to a simple conclusion: if SSBs are capable of autonomously balancing their profile across the 3 phases (3Φ controllable elements), the DSO can reliably manage its system using solely 1Φ network equivalents. The predecessor would be suitable for networks that host customers with limited capabilities for local phase balancing.

F. Robustness Against Communication Failures

Even though this work assumes that the DSO-SSB communication is perfect, it is useful to perform a *preliminary* exploration of the approach's robustness against communication failures. Table VIII presents how the objective function is impacted (ancillary and violation costs) when, throughout the entire day, any one of the DSO's 24 time-step requests may fail to reach their proper recipient. Despite not having explicitly considered the issue, the approach is naturally resilient against these issues. The main reason is the optimization horizon length and granularity: first, the network does not experience huge *unforeseen* changes. Second, SSBs plan so far ahead, that they always have access to pre-set, nigh-optimal operational settings. The network is thus able to comfortably cope with communication issues, even under extreme conditions. The objective function increases by 0.59% and 0.87% for the passive and active schemes respectively, owing mostly due to moving to penalization zones *at the start of the day*, when sufficient long-term planning has not been established yet. The increase in violations is next to zero. Shorter optimization horizons or higher failure probabilities would have a stronger impact. However, the default choices are in fact reasonable.

G. Scalability Aspects

With some exceptions, LV networks are commonly characterized by a small number of nodes and low controllability, the customers corresponding to an MV-LV substation usually

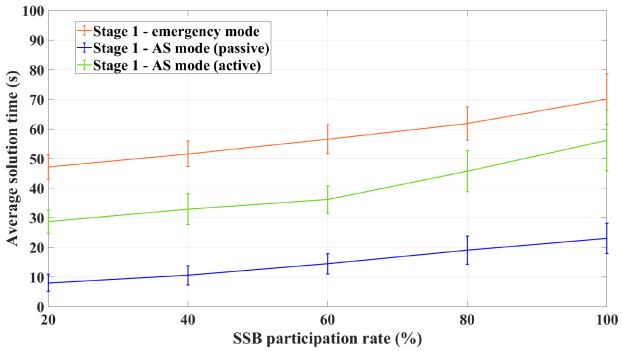

Fig. 8. U.K. network average solution times & standard deviation, stage 1, 12-step horizon.

numbering in the dozens [40]; the size of any optimization problem is, in general, less restrictive than in MV networks. However, to demonstrate applicability to a wider range of real-life settings, we examine the behavior of an actual LV network when governed by the proposed approach. The U.K.-based, 4-feeder network comprises 400 nodes (post-merging) and 200 customers [40]. While the 1Φ representation is again used for stage 1, network and customer imbalances are, like before, considered in stages 2, 3, as well as in the 3Φ validation. We assume a varying SSB participation rate, from 20% to 100%.

The results of the experiments above are presented in Fig. 8, from which once can observe that even for a much larger network, both the NLP module and MILP module scale up very well. The solution times are indeed noticeably higher (3-5 times higher), but still remain practical for the fine granularity of 15-min intervals. Naturally, higher SSB participation rates slow down the solution time (more control variables), but not to a substantial degree; this follows the conclusions that were drawn in the authors' previous work [29]. In line with all previous observations, the passive scheme remains the faster module, clocking in between 10-20 seconds, on average. The active scheme is more complex and thus slower (30-50 seconds), but is still comfortably handled by the powerful CPLEX solver. Even the slowest module, i.e., the NLP emergency mode, requires 80 seconds at worst to solve (highest participation rate, highly stressed system), at no point hindering the reliable application of the proposed approach. All recorded solution times are less than 2 minutes, meaning they remain well-suited for the 15-min granularity (an even finer granularity could perhaps be feasible, at least under the prevailing assumptions about the network and customers). These results, corroborated with those in Section IV-C, empirically demonstrate that the methodology can scale up to a wider range of LV network sizes and controllable SSBs.

V. DISCUSSION AND IMPLEMENTATION CONSIDERATIONS

A. Practical Considerations

Important observations were made with respect to the potential of LV networks acquiring an elevated role in the future smart grid era, specifically with regard to the coordination of SSBs to provide AS support to the MV network. Despite the promise of the proposed approach, one must, however, not forget the practical considerations that would make it possible.

Coordinating SSBs through targeted requests presupposes knowledge of the network's layout (realistic), sufficient information for state estimation (smart meters, forecasting software), SSB energy management systems, and adequate DSO-SSB communication infrastructure (still not attained). The penalization zones of each scheme must be carefully selected; the sensitivity analysis is a good starting point. The DSO would need to be actively involved in LV network management. If SSBs provide adequate phase balancing, the proposed approach performs similarly to its idealized version of [3]. However, aside from the capability of controlling each phase, SSBs should be equipped with the less common and more expensive 3Φ inverters. The commonplace 1Φ inverters may often fail to cope with a network's flexibility demands, leading to much higher management costs [29]. However, they are currently the dominant kind of device in most buildings.

B. Mathematical Modeling Considerations

When employing linearizations in AS mode, the quality of the solution is not significantly affected. However, "problematic" flows can still be observed in highly loaded networks at non-emergency states, possibly leading to operating states with lingering violations. The linearizations could rely less on a generic methodology and instead be constructed to address the specific needs of the problem. Also, more sophisticated methods for choosing vector ι^* may be required, depending on the complexity of the application. The most appropriate linearization when expanding to 3Φ models demands additional exploration. Constructing a 3Φ version of the current linearization is an option; so is opting for an already established, explicit 3Φ linearization. Since the employed linearization was not originally designed for LV networks, the latter option might be preferable; this of course requires further research.

It was demonstrated that even in common, practical real-life test cases, i.e., 15-min granularity analysis for LV networks hosting up to 200 customers, the proposed approach is reliably scalable. However, for the largest multi-feeder LV networks hosting several hundreds of customers, and for an even finer horizon granularity, the approach may not be practical *in its current form*. To expand to these uncommon, large-scale cases, one option would be to also approximate the NLP model stemming from the emergency mode. Another alternative would be to apply the methodology to the single-feeder level and subsequently engage in cross-feeder information exchange at the coupling point in order to determine the global behavior of the LV network; inspiration could easily be drawn from mainstream techniques for decentralized optimization. The optimal choices remain the subject of future work.

C. Network-Driven vs Price-Driven Approaches

Price-driven network management is a highly prominent concept, involving the DSO using price signals to manage its system, within some market framework. The proposed approach for network management and AS provision to the MV network could, conceptually, be amendable to a price-driven one, should the costs C_1-C_6 be considered as dynamic. This is more akin to the mentality that flexibility utilization in LV networks should be market-driven. However, while more customer-friendly, one should also be wary of the inherent weaknesses in price-driven network management.

The biggest issue is constructing the necessary market environment for the envisioned SSB participation [41], [42], [43]. This is a hard undertaking, the technical and legal complexity being immense. Moreover, eliciting specific end-user behaviors is not an exact science; especially when pursuing complex network-wide objectives (e.g., AS provision) allowing too much leeway can lead to unpredictable results. For example, because many approaches allow market participation only above a certain size [44], large players can collude or dominate proceedings, manipulating the network and gauging the DSO for exorbitant financial rewards. The issues of fairness and manageable network behavior should also not be underplayed. Most price-driven approaches assume that the network is only lightly stressed, or, in the opposite case, may unfairly penalize large and electrically distant end-users. Contrary to this work, few researchers have addressed the necessity of financial incentives for i) imbalance mitigation, ii) specific-request compliance, or iii) automatic re-assignment of missing flexibility. While price-driven approaches are an interesting alternative, designing a market framework that would also allow for the reliable pursuit of complex, network-specific objectives, is a difficult task.

D. Exact vs Relaxed Models

The nature of the examined applications (LV network, 1Φ representation) precludes too restrictive problem sizes. The conscious choice was thus made to go with exact (NLP) or approximated (MILP) network models. How well relaxed 3Φ network models would have fared is, however, a reasonable question. As described hereafter, in the vast majority of cases, the relaxations in unbalanced networks are not tight, which usually leads to non-meaningful solutions. The mathematical requirements are difficult to satisfy in realistic power systems [45]. A feasible, at least locally optimal solution was deemed preferable to risking a relaxed, yet physically meaningless one.

It is worth discussing the limitations of relaxations for the specific application. In short, the two most prominent relaxation "schools" in unbalanced distribution systems are second-order cone programming (SOCP) and semidefinite programming (SDP). The relevant tightness of the SOCP relaxation, either in its generic form [46] or in its more advanced, mixed-integer representation [47], ultimately hinges on the assumption that the upper limits for nodal active and reactive power are unconstrained. However, there is currently no real power system (be that transmission or distribution) for which this assumption would hold; the optimality gap for unbalanced SOCP problems is in general always positive [45]. Experience has shown that the SDP relaxation is in general tighter. However, even works that popularized its use refrain from dubbing it exact. The seminal paper [48] in fact provided no mathematical proof of tightness, offering an intuitive argument and a small-scale example of why the relaxation should, *empirically*, be exact. Even advanced versions, e.g.,

the chordal relaxation [49], often fail to converge to a global optimum for the relaxed feasible space; the proposed strategies for dealing with such instances have also demonstrated significant weaknesses. In light of the above, the authors opted for avoiding these issues altogether.

E. Alignment With the "Smart Grid Vision"

There is currently a lively debate on whether control approaches in LV networks should be universal, i.e., customer-independent, or tailor-made, i.e., customer-dependent. The older-school approach to network management was that customer would be mostly passive, and that the DSO would employ its own tools to counteract the customer-driven decisions that threatened network's operation. When adopting this research avenue, any developed methodology should explicitly consider the issue of imbalance mitigation; the discussion in Sections V-A–V-D serves as a solid starting point.

A fundamental assumption of this work, in line with the "smart grid vision" [33], is that the DSO will not directly control LV networks, but will instead rely on a cooperation framework with its customers; demand-response programs are a classic example of an application within the scope of "cooperation". A weakness of said framework is that, at times, it depends on end-users capabilities to support proper network operation, and if an approach is designed independently, there is a danger of failing to reliably implement it. As such, when designing any approach to combat specific issues (in our case, network imbalance), it is of vital importance that said approach has a solid basis for implementation; Eq. (19) can be thought of as a crude version of an envisioned financial tool to motivate the desired behavior. Again, the assumption is that end-users are in fact capable of responding to the DSO's signals.

VI. Conclusion and Future Research

The potential of LV networks for providing AS to the MV level (in support of and as part of the DSO-TSO cooperation), while at the same time managing any potential technical issues, was explored in substantial detail through successfully applied active and passive schemes. While the passive one is simpler and suitable for any LV network, the active one is more lucrative (financial rewards) and recommended for networks with the capability to reliably sustain it. As distribution systems become more involved in the management of power grids (through the envisioned TSO-DSO coordination), MV systems should focus more on their cooperation with transmission systems rather than constant self-management. As was demonstrated, LV networks can, through DSO-SSB coordination, design reliable strategies for supporting MV networks by providing various kinds of AS in a scalable manner, while combating internal issues. A novel 3-stage approach based on DSO-SSB coordination was the catalyst for optimizing the behavior of all involved players.

Through the proposed 3-stage approach, the DSO can make targeted 1Φ requests to SSBs, which in turn a) produce an effective 3Φ-equivalent solution, and b) automatically support SSBs that at times run out of flexibility. However, despite the performance of the proposed approach, i.e., fast solution times, approximated solutions of good quality and compliance with real-time application requirements, future research could be focused on guaranteeing feasible solutions at all times, rather than depending exclusively on SSBs (phase balancing). The robustness against typical communication failure scenarios is solid, but could be further improved to address more complex latency cases. While the focus was on AS for voltage control support, the approach could expand to include congestion-related AS, if need be; this is left as future work by the authors.

Appendix

A. Reformulation of Passive Ancillary Objective

The objective (7) is reformulated through the following steps: The penalty is always non-negative (45). The penalty is not activated if either of $\Psi^{\mathrm{p}}, \Psi^{\phi}$ are active (46). In case both binaries are inactive, the penalty must be activated, while accounting for the sign of $|Q^{\mathrm{ex}}|$; this is achieved through (47), which is in convex closed form. The left side of (9) is also in convex closed form. The right side requires an auxiliary binary variable ζ, reformulating to (48)-(49):

$$F_3^{\mathrm{pass}} \geq 0 \tag{45}$$

$$F_3^{\mathrm{pass}} \leq M^{\mathrm{p}} \cdot \left(1 - \Psi^{\mathrm{p}}\right) \quad \& \quad F_3^{\mathrm{pass}} \leq M^{\mathrm{p}} \cdot \left(1 - \Psi^{\phi}\right) \tag{46}$$

$$\frac{F_3^{\mathrm{pass}}}{C^{\mathrm{P}}} + Q^{\mathrm{lim}} + \frac{M^{\mathrm{p}}}{C^{\mathrm{P}}} \cdot \left(\Psi^{\mathrm{p}} + \Psi^{\phi}\right) \geq \left|Q^{\mathrm{ex}}\right| \tag{47}$$

$$Q^{\mathrm{ex}} + M^{\zeta} \cdot \zeta \geq Q^{\mathrm{lim}} - M^{\mathrm{p}} \cdot \Psi^{\phi} \tag{48}$$

$$-Q^{\mathrm{ex}} + M^{\zeta} \cdot (1 - \zeta) \geq Q^{\mathrm{lim}} - M^{\mathrm{p}} \cdot \Psi^{\phi}. \tag{49}$$

B. Reformulation of Active Ancillary Objective

The objective (12) is reformulated through the following steps: recalling that when $\Psi^{\mathrm{q}}, \Psi^{\mathrm{v}}$ are identical the network is compliant, the bilinearity can be lifted according to (50)-(52):

$$\max\left\{\Psi^{\mathrm{q}}, \Psi^{\mathrm{v}}\right\} - \min\left\{\Psi^{\mathrm{q}}, \Psi^{\mathrm{v}}\right\} = Y \tag{50}$$

$$F_3^{\mathrm{act}} \geq C_3^{\mathrm{x}} \cdot \left|Q^{\mathrm{ex}}\right| - M^{\mathrm{v}} \cdot (1 - Y) \tag{51}$$

$$F_3^{\mathrm{act}} \geq -C_3^{\checkmark} \cdot \left|Q^{\mathrm{ex}}\right| - M^{\mathrm{v}} \cdot Y \tag{52}$$

The non-convex (52) is reformulated with the help of the auxiliary binary variable ρ, according to (53)-(54):

$$Q^{\mathrm{ex}} + M^{\rho} \cdot \rho \geq \left(C_3^{\checkmark}\right)^{-1} \cdot \left(-F_3^{\mathrm{act}} - M^{\mathrm{v}} \cdot Y\right) \tag{53}$$

$$-Q^{\mathrm{ex}} + M^{\rho} \cdot (1 - \rho) \geq \left(C_3^{\checkmark}\right)^{-1} \cdot \left(-F_3^{\mathrm{act}} - M^{\mathrm{v}} \cdot Y\right) \tag{54}$$

The final step is to remove the min, max operators. Even though there is a mathematically equivalent procedure (involving 5 binary variables), one can instead exploit the nature of the optimization problem to our advantage. The auxiliary variables $\Lambda^{\mathrm{min}}, \Lambda^{\mathrm{max}}$ are defined, constrained according to (56), (57), which are designed to represent the min, max operators. The variable Y is re-defined according to (55).

$$Y = \Lambda^{\mathrm{max}} - \Lambda^{\mathrm{min}} \tag{55}$$

$$\Lambda^{\mathrm{min}} \leq \Psi^{\mathrm{q}} \quad \& \quad \Lambda^{\mathrm{min}} \leq \Psi^{\mathrm{v}} \tag{56}$$

$$\Lambda^{\mathrm{max}} \geq \Psi^{\mathrm{q}} \quad \& \quad \Lambda^{\mathrm{max}} \geq \Psi^{\mathrm{v}} \tag{57}$$

Now, (50) and (55)-(57) are not mathematically equivalent; there exist cases where the latter can treat compliance as non-compliance ($\Psi^{\mathrm{q}} = \Psi^{\mathrm{v}} = 0$ but $\Lambda^{\max} = 1$, or $\Psi^{\mathrm{q}} = \Psi^{\mathrm{v}} = 1$ but $\Lambda^{\min} = 0$). However, such a case will needlessly **increase** the value of the objective function. Despite being *feasible*, the solver will deem these instances as sub-optimal and promptly reject them. Due to the nature of the problem, this approach is expected to return the same results as its mathematical equivalent.

REFERENCES

[1] A. J. Marszal *et al.*, "Zero energy building—A review of definitions and calculation methodologies," *Energy Build.*, vol. 43, no. 4, pp. 971–979, 2011.

[2] I. I. Avramidis, F. Capitanescu, and G. Deconinck, "A generic multi-period optimal power flow framework for combating operational constraints via residential flexibility resources," *IET Gener. Transm. Distrib.*, vol. 15, no. 2, pp. 306–320, 2021.

[3] I. Avramidis, V. Evangelopoulos, F. Capitanescu, P. Georgilakis, and G. Deconinck, "Predictive control in LV networks: A 3-stage approach for smart sustainable buildings," in *Proc. IEEE Powertech Madrid*, Jun. 2021, pp. 1–9.

[4] A. Saint-Pierre and P. Mancarella, "Active distribution system management: A dual-horizon scheduling framework for DSO/TSO interface under uncertainty," *IEEE Trans. Smart Grid*, vol. 8, no. 5, pp. 2186–2197, Sep. 2017.

[5] D. B. Arnold, M. D. Sankur, M. Negrete-Pincetic, and D. S. Callaway, "Model-free optimal coordination of distributed energy resources for provisioning transmission-level services," *IEEE Trans. Power Syst.*, vol. 33, no. 1, pp. 817–828, Jan. 2018.

[6] M. Rossi *et al.*, "TSO-DSO coordination to acquire services from distribution grids: Simulations, cost-benefit analysis and regulatory conclusions from the SmartNet project," *Electr. Power Syst. Res.*, vol. 180, Dec. 2020, Art. no. 106700.

[7] J. Silva *et al.*, "Estimating the active and reactive power flexibility area at the TSO-DSO interface," *IEEE Trans. Power Syst.*, vol. 33, no. 5, pp. 4741–4750, Sep. 2018.

[8] S. Riaz and P. Mancarella, "On feasibility and flexibility operating regions of virtual power plants and TSO/DSO interfaces," in *Proc. IEEE Powertech Milan*, Jun. 2019, p. 9.

[9] P. Cuffe, P. Smith, and A. Keane, "Capability chart for distributed reactive power resources," *IEEE Trans. Power Syst.*, vol. 29, no. 1, pp. 15–22, Jan. 2014.

[10] H. Nosair and F. Bouffard, "Flexibility envelopes for power system operational planning," *IEEE Trans. Sustain. Energy*, vol. 6, no. 3, pp. 800–809, Jul. 2015.

[11] A. Vicente-Pastor, J. Nieto-Martin, D. W. Bunn, and A. Laur, "Evaluation of flexibility markets for retailer-DSO–TSO coordination," *IEEE Trans. Power Syst.*, vol. 34, no. 3, pp. 2003–2012, May 2019.

[12] S. Stankovic and L. Sö, "Probabilistic reactive power capability charts at DSO/TSO interface," *IEEE Trans. Smart Grid*, vol. 11, no. 5, pp. 3860–3870, Sep. 2020.

[13] A. Oulis-Rousis *et al.*, "Provision of voltage ancillary services through enhanced TSO-DSO interaction and aggregated distributed energy resources," *IEEE Trans. Sustain. Energy*, vol. 12, no. 2, pp. 897–908, Apr. 2021.

[14] A. G. Givisiez *et al.*, "A review on TSO-DSO coordination models and solution techniques," *Electr. Power Syst. Res.*, vol. 180, Dec. 2020, Art. no. 106659.

[15] A. Shahsavari *et al.*, "Distribution grid reliability versus regulation market efficiency: An analysis based on micro-PMU data," *IEEE Trans. Smart Grid*, vol. 8, no. 6, pp. 2916–2925, Nov. 2017.

[16] G. Tsaousoglou, J. S. Giraldo, P. Pinson, and N. G. Paterakis, "Mechanism design for fair and efficient DSO flexibility markets," *IEEE Trans. Smart Grid*, vol. 12, no. 3, pp. 2249–2260, May 2021.

[17] F.L. Müller, J. Szabó, O. Sundström, and J. Lygeros, "Aggregation and disaggregation of energetic flexibility from distributed energy resources," *IEEE Trans. Smart Grid*, vol. 10, no. 2, pp. 1205–1214, Mar. 2019.

[18] N. Savopoulos and N. Hatziargyriou, "Estimating operational flexibility from active distribution grids," in *Proc. 17th Int. Conf. Eur. Energy Market*, Sep. 2020, pp. 1–6.

[19] E. Polymeneas and S. Meliopoulos, "Aggregate modelling of distribution systems for multi-period OPF," in *Proc. IEEE Powertech Eindhoven*, Jun. 2015, pp. 1–9.

[20] B. Olek and M. Wierzbowski, "Local energy balancing and ancillary services in low voltage networks with distributed generation, energy storage and active loads," *IEEE Trans. Ind. Electron.*, vol. 62, no. 4, pp. 2499–2508, Apr. 2015.

[21] A. Asrari, M. Ansari, J. Khazaei, and P. Farji, "A market framework for decentralized congestion management in smart distribution grids considering collaboration among electric vehicle aggregators," *IEEE Trans. Smart Grid*, vol. 11, no. 2, pp. 1147–1158, Mar. 2020.

[22] V. Rigoni, D. Flynn, and A. Keane, "Coordinating demand response aggregation with LV network operational constraints," *IEEE Trans. Power Syst.*, vol. 36, no. 2, pp. 979–990, Mar. 2021.

[23] M. Zerva and M. Geidl, "Contribution of active distribution grids to the coordinated voltage control of the swiss transmission system," in *Proc. Power Syst. Comput. Conf.*, Aug. 2014, pp. 1–8.

[24] S. Karagiannopoulos *et al.*, "Active distribution grids offering ancillary services in islanded and grid-connected mode," *IEEE Trans. Smart Grid*, vol. 11, no. 1, pp. 623–633, Jan. 2020.

[25] F. Lamberti, V. Calderaro, V. Galdi, and A. Piccolo, "Ancillary services provided by residential ESSs in LV networks: Assessing the opportunity costs," in *Proc. IEEE Powertech Manchester*, Jun. 2017, pp. 1–8.

[26] S. Karagiannopoulos, C. Mylonas, P. Aristidou, and G. Hug, "Active distribution grids providing voltage support: The Swiss case," *IEEE Trans. Smart Grid*, vol. 12, no. 1, pp. 268–278, Jan. 2021.

[27] L. Gutierrez-Lagos, K. Petrou, and L. F. Ochoa, "Quantifying the effects of MV-LV distribution network constraints and DER reactive power capabilities on aggregators," *IET Gener. Transm. Distrib.*, vol. 15, no. 14, pp. 2019–2032, 2021.

[28] J.R. Aguero, E. Takayesu, D. Novosel, and R. Masiello, "Modernizing the grid: Challenges and opportunities for a sustainable future," *IEEE Power Energy Mag.*, vol. 15, no. 3, pp. 74–83, May/Jun. 2017.

[29] I.I. Avramidis, F. Capitanescu, and G. Deconinck, "A comprehensive multi-period optimal power flow framework for smart LV networks," *IEEE Trans. Power Syst.*, vol. 36, no. 4, pp. 3029–3041, Jul. 2021.

[30] O. Erdinc *et al.*, "Smart household operation considering bi-directional EV and ESS utilization by real-time pricing-based DR," *IEEE Trans. Smart Grid*, vol. 6, no. 3, pp. 1281–1291, May 2015.

[31] *Study on the Future Design of the Ancillary Service of Voltage and Resactive Power Control*, Belgian Transm. Syst. Oper., Elia, Brussels, Belgium, 2018.

[32] G. Valverde, D. Shchetinin, and G. Hug, "Coordination of distributed reactive power sources for voltage support of transmission networks," *IEEE Trans. Sustain. Energy*, vol. 10, no. 3, pp. 1544–1553, Jul. 2019.

[33] H. Farhangi, "The path of the smart grid," *IEEE Power Energy Mag.*, vol. 8, no. 1, pp. 18–28, Jan./Feb. 2010.

[34] Z. Yang *et al.*, "A linearized OPF model with reactive power and voltage magnitude: A pathway to improve the MW-only DC OPF," *IEEE Trans. Power Syst.*, vol. 33, no. 2, pp. 1734–1745, Mar. 2018.

[35] L. Gutierrez-Lagos, M. Z. Liu, and L. F. Ochoa, "Implementable three-phase OPF formulations for MV-LV distribution networks: MILP and MIQCP," in *Proc. IEEE ISGT Latin America*, Sep. 2015, pp. 1–8.

[36] S. Weckx and J. Driesen, "Load balancing with EV chargers and PV inverters in unbalanced distribution grids," *IEEE Trans. Sustain. Energy*, vol. 6, no. 2, pp. 635–643, Apr. 2015.

[37] K. Strunz *et al.*, "Benchmark systems for network integration of renewable and distributed energy resources," in *Proc. CIGRE*, 2014, pp. 4–6.

[38] *Provision of Customers Based on Synthetic Profiles*. Accessed: Mar. 15, 2021. [Online]. Available: https://creos-net.lu/fournisseurs/electricite/profils-synthetiques.html

[39] *Photovoltaic Geographical Information System*. Accessed: Mar. 15, 2021. [Online]. Available: https://re.jrc.ec.europa.eu/pvg/_tools/en/tools.html

[40] A. Navarro-Espinosa and L. F. Ochoa, "Probabilistic impact assessment of low carbon technologies in LV distribution systems," *IEEE Trans. Power Syst.*, vol. 31, no. 3, pp. 2192–2203, May 2016.

[41] P. H. Divshali and D. Shereck, "Multi-agent transactive energy management system considering high levels of renewable energy source and electric vehicles," *IET Gener. Transm. Distrib.*, vol. 11, no. 15, pp. 3713–3721, 2017.

[42] J. C. Bedoya, M. Ostadijafari, C. C. Liu, and A. Dubey, "Decentralized transactive energy for flexible resources in distribution systems," *IEEE Trans. Sustain. Energy*, vol. 12, no. 2, pp. 1009–1019, Apr. 2021.

[43] T. Wei, Q. Zhu, and N. Yu, "Proactive demand participation of smart buildings in smart grid," *IEEE Trans. Comput.*, vol. 65, no. 5, pp. 1392–1406, May 2016.
[44] M. Ostadijafari, A. Dubey, and N. Yu, "Linearized price-responsive HVAC controller for optimal scheduling of smart building loads," *IEEE Trans. Smart Grid*, vol. 11, no. 4, pp. 3131–3145, Jul. 2020.
[45] K. Christakou, D.-C. Tomozei, J.-Y. L. Boudec, and M. Paolone, "ACOPF in radial distribution networks—Part I: On the limits of the branch flow convexification and the alternating direction method of multipliers," *Electr. Power Syst. Res.*, vol. 143, pp. 438–450, Feb. 2017.
[46] M. Farivar and S. H. Low, "Branch flow model: Relaxations and convexification-Parts I & II," *IEEE Trans. Power Syst.*, vol. 28, no. 3, pp. 2554–2572, Aug. 2013.
[47] L. H. Macedo, J. F. Franco, M. J. Rider, and R. Romero, "Optimal operation of distribution networks considering energy storage devices," *IEEE Trans. Smart Grid*, vol. 6, no. 6, pp. 2825–2836, Nov. 2015.
[48] E. Dall'Anese, H. Zhu, and G. B. Giannakis, "Distributed optimal power flow for smart microgrids," *IEEE Trans. Smart Grid*, vol. 4, no. 3, pp. 1464–1475, Sep. 2013.
[49] W. Wang and N. Yu, "Chordal conversion based convex iteration algorithm for three-phase optimal power flow problems," *IEEE Trans. Power Syst.*, vol. 32, no. 2, pp. 1603–1613, Mar. 2018.

Iason-Iraklis Avramidis (Student Member, IEEE) received the Dipl.- Ing degree in electrical and computer engineering from the National Technical University of Athens, Greece, in 2017, and the M.Sc. degree in energy science and technology from ETH Zurich, Switzerland, in 2019. He is currently pursuing the Ph.D. degree with the Electrical Energy & Computer Architecture Group, KU Leuven, Belgium. He is currently with the Environmental Research and Innovation, Luxembourg Institute of Science and Technology. His research interests include the optimization of smart and sustainable distribution grids, local flexibility markets, and security-constrained optimal power flow.

Florin Capitanescu (Member, IEEE) received the Electrical Power Engineering degree from the University "Politehnica" of Bucharest, Romania, in 1997, and the Ph.D. degree from the University of Liège, Belgium, in 2003. Since 2015, he has been with the Environmental Research and Innovation, Luxembourg Institute of Science and Technology as a Senior R&T Associate. His main research interests include the application of optimization methods to operation of transmission and active distribution systems, particularly security-constrained optimal power flow approaches, voltage instability, and smart sustainable buildings.

Vasileios A. Evangelopoulos received the Diploma degree in electrical and computer engineering and the M.Sc. degree in engineering-economic systems from National Technical University of Athens, Greece, in 2013, where he is currently pursuing the Ph.D. degree with the School of Electrical and Computer Engineering. His research interests include power systems optimization techniques, distributed energy resources and flexible management of active distribution systems. He is a member of the Technical Chamber of Greece.

Pavlos S. Georgilakis (Senior Member, IEEE) received the Diploma and Ph.D. degrees in electrical and computer engineering from National Technical University of Athens (NTUA), Athens, Greece, in 1990 and 2000, respectively. In September 2009, he joined as a Faculty Member with the School of Electrical and Computer Engineering, NTUA, where he has been an Associate Professor since August 2018. His current research interests include optimization algorithms and computational intelligence techniques for the optimal operation and planning of smart distribution systems. He is a member of the Technical Chamber of Greece.

Geert Deconinck (Senior Member, IEEE) received the M.Sc. degree in electrical engineering and the Ph.D. degree in engineering sciences from KU Leuven, Belgium, in 1991 and 1996, respectively, where he is a Full Professor (gewoon hoogleraar). He is the Head of the Research Group on Electrical Energy Systems and Application (ESAT), KU Leuven and the EnergyVille Researc Center. His research focuses on robust distributed coordination and control, specifically in the context of smart grids. He is a Fellow of the Institute of Engineering and Technology.